

AREA-PRESERVING GEOMETRIC HERMITE INTERPOLATION

GEOFFREY MCGREGOR AND JEAN-CHRISTOPHE NAVE

ABSTRACT. In this paper we establish a framework for geometric interpolation with exact area preservation using Bézier cubic polynomials. We show there exists a family of such curves which are 5th order accurate, one order higher than standard geometric Hermite interpolation. We prove this result is valid when the curvature at the endpoints does not vanish, and in the case of vanishing curvature, the interpolation is 4th order accurate. The method is computationally efficient and prescribes the parametrization speed at endpoints through an explicit formula based on the given data. Additional accuracy (i.e. same order but lower error constant) may be obtained through an iterative process to find optimal parametrization speeds which further reduces the error while still preserving the prescribed area exactly.

1. INTRODUCTION

In the last several decades, interpolation using parametric curves has been studied extensively with the primary application being geometric design and computer graphics [2, 3, 4, 9, 10]. The class of parametric polynomials we are concerned with here are continuous in both the position and velocity vectors. These curves are classified as G^1 , or geometric continuity of order 1. Further discussion of parametric and geometric continuity can be found in [1].

In this paper we introduce a G^1 Bézier cubic interpolation framework which, given a parametric curve $\langle f(s), g(s) \rangle \in \mathbb{R}^2$, with $s \in [s_0, s_1]$, exactly matches the area $\int_{s_0}^{s_1} g(\tau)f'(\tau)d\tau$. A conservative framework of this type may be of particular interest in areas of mathematics and engineering where physical laws must be obeyed, for examples see [13]. In addition to being consistent with physical principles, conservative schemes offer additional stability properties [18]. From the outset, conservative methods of this type may not directly appeal to the geometric design community, however the results presented in this paper show it performs advantageously when compared to standard non-conservative methods, such as the curvature matching method described in [2] and the curvature variation energy method discussed in [11]. One interesting finding of our work is that requiring a traditionally 4th order Bézier cubic to exactly match the area of a target function results in a 5th order accurate interpolating polynomial. In fact, we show that

Date: October 3, 2018.

2000 Mathematics Subject Classification. 68Q25, 68R10, 68U05.

Key words and phrases. Parametric curves, geometric interpolation, area-preserving interpolation, structure preserving interpolation, Bézier curves.

The research of GMc was supported in part by a Schulich Scholarship at McGill University.

The research of JCN was supported in part by the NSERC Canada Discovery Grants Program. Additionally, JCN would like to thank the Shanghai Jiaotong University Institute of Natural Sciences for hosting him while completing this work.

there is an entire family of area-preserving G^1 cubic polynomials which are 5th order accurate. In many applications choosing any member of this family will provide sufficient accuracy, however, in situations where high precision is valued, an optimal member of the family may be selected through an iterative procedure. We discuss details of the optimization procedure and show that the error can be further reduced by several orders of magnitude. Before introducing the area-preserving method, we discuss a selection of relevant results from the geometric design and interpolation literature.

Geometric interpolation was first introduced by de Boor et al. in [2]. In that work a parametric-cubic interpolation framework matching function value, tangents and curvature at endpoints was derived. This is now classified as G^2 interpolation and is 6th order accurate. The method reduces to 4th order if the curvature vanishes anywhere within the interpolation domain. Since that seminal result, work in geometric interpolation has grown extensively, with an emphasis on non-local quantities. For example, in [5], the author succeeded to create a G^1 interpolation framework which matches prescribed arclength using Pythagorean-hodograph (PH) curves. For more on PH curves see [6, 7, 8]. Other extensively studied methods of interpolation are concerned with seeking G^1 polynomial curves which minimize the strain energy, $\int_{t_0}^{t_1} (\kappa(t))^2 dt$, where $\kappa(t)$ denotes the curvature, or the curvature variation energy $\int_{t_0}^{t_1} (\kappa'(t))^2 dt$. For example, Jaklic and Zagar in [12] study G^1 cubic polynomials which minimize an approximate strain energy, also called the linearized bending energy. This is also studied in [19] and extended to quintics in [14]. In [11] Jaklic and Zagar present a 4th order accurate G^1 interpolation method which minimizes a functional approximating the curvature variation energy. Recently in [15], Lu et al. introduced a scheme which computes G^1 cubic interpolants minimizing the true curvature variation energy through a constrained minimization problem. The results are concluded to be better than the approximate methods in [11], however this additional accuracy comes with a significant increase in computational cost. After an extensive search, it is to the best of our knowledge that area-preservation within the context of parametric interpolation is novel. In the results section we will compare our area-preserving G^1 interpolation method to the curvature matching method of de Boor et al. and the approximate curvature variation energy method of Jaklic and Zagar.

We begin section 2 with a brief discussion of Bézier cubics and introduce the area-preserving Bézier cubic framework. We then prove two Lemmas which lead to the main Theorem stating that a certain class of area-preserving Bézier cubics are 5th order accurate. The main Theorem is followed by a Corollary which states that no 6th order method can be constructed within this framework. In section 3 numerical experiments are conducted to compare the area-preserving scheme to other geometric interpolation methods, while also verifying the results presented in section 2. We then discuss the optimized method and show that an increase in accuracy can be achieved by choosing an optimal member of the area-preserving Bézier cubic family. In section 4 we give some concluding remarks and discuss future directions of work.

2. AREA-PRESERVING BÉZIER CUBICS

A parametric Bézier cubic $\vec{B}(t) = \langle B_1(t), B_2(t) \rangle$ interpolating point \vec{A} to point \vec{D} , for $\vec{A}, \vec{D} \in \mathbb{R}^2$, is given by

$$(2.1) \quad \vec{B}(t) = \vec{A}(1-t)^3 + 3\vec{C}_1(1-t)^2t + 3\vec{C}_2(1-t)t^2 + \vec{D}t^3, \quad \text{for } t \in [0, 1],$$

where \vec{C}_1 and \vec{C}_2 are referred to as control points which dictate the tangent direction and magnitude of \vec{B} at $t = 0$ and $t = 1$. The tangent direction at endpoints will be extracted from the prescribed data, therefore, the remaining degrees of freedom are the magnitudes, r_1 and r_2 , for the left and right tangents respectively. Taking the tangent direction at the left endpoint to be $\vec{\alpha}$ and $\vec{\beta}$ on the right we therefore obtain

$$\vec{B}'(0) = r_1\vec{\alpha} \quad \text{and} \quad \vec{B}'(1) = r_2\vec{\beta}.$$

Rewriting the control points in terms of $\vec{A}, \vec{D}, \vec{\alpha}, \vec{\beta}, r_1$ and r_2 , yields the two-parameter family of Bézier cubics matching function value and tangent directions, (2.2)

$$\vec{B}(t) = \vec{A}(1-t)^3 + 3\left(\vec{A} + \frac{r_1\vec{\alpha}}{3}\right)(1-t)^2t + 3\left(\vec{D} - \frac{r_2\vec{\beta}}{3}\right)(1-t)t^2 + \vec{D}t^3, \quad \text{for } t \in [0, 1].$$

Given a parametric curve $\langle F(s), g(s) \rangle$ parametrized by $s \in [s_0, s_1]$, we reduce the two-parameter family of solutions (2.2) to a one-parameter family by imposing the the parametric area condition

$$(2.3) \quad \int_0^1 B_2(t)B_1'(t)dt = \int_{s_0}^{s_1} g(s)F'(s)ds.$$

Using that Bézier curves are formed by generalized convex combinations, we simplify the expression by shifting \vec{A} to the origin, which yields

$$(2.4) \quad \begin{aligned} \vec{B}(t) - \vec{A} &= \vec{B}(t) - \vec{A}((1-t)^3 + 3(1-t)^2t + 3(1-t)t^2 + t^3) \\ &= r_1\vec{\alpha}(1-t)^2t + 3\left(\vec{D}^* - \frac{r_2\vec{\beta}}{3}\right)(1-t)t^2 + \vec{D}^*t^3, \quad \text{for } t \in [0, 1], \end{aligned}$$

where $\vec{D}^* = \vec{D} - \vec{A}$, but for convenience we will drop the *. Using the shifted form (2.4), the parametric area (2.3) formula becomes

$$(2.5) \quad \int_0^1 B_2(t)B_1'(t)dt = \frac{r_1r_2}{60}(\vec{\alpha} \times \vec{\beta}) + \frac{r_1}{10}(\vec{D} \times \vec{\alpha}) + \frac{r_2}{10}(\vec{\beta} \times \vec{D}) + \frac{D_1D_2}{2} = \mathcal{C},$$

where \mathcal{C} is the prescribed area after shifting the left endpoint to the origin. Note that shifting $\langle F(s), g(s) \rangle$ to $\langle F(s) - x_0, g(s) - y_0 \rangle$, yields $\mathcal{C} = \int_{s_0}^{s_1} g(s)F'(s)ds - y_0(F(s_1) - F(s_0))$. Returning to equation (2.5), and moving $\frac{D_1D_2}{2}$ to the right hand side, we obtain the area constraint equation

$$(2.6) \quad \frac{r_1r_2}{60}(\vec{\alpha} \times \vec{\beta}) + \frac{r_1}{10}(\vec{D} \times \vec{\alpha}) + \frac{r_2}{10}(\vec{\beta} \times \vec{D}) = \mathcal{C}_R,$$

prescribing the signed area about the secant line of the parametric polynomial \vec{B} to equal that of the data. A sketch of the prescribed signed area is given in Figure 1.

Our goal is as follows: Given the signed area \mathcal{C}_R , we aim to find choices of $r_1 > 0$ and $r_2 > 0$ which satisfy equation (2.6), and in addition, obtain an estimate for the

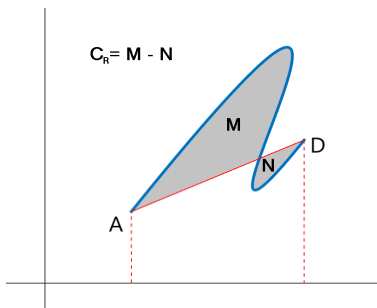


FIGURE 1. Signed area about the secant line between \vec{A} and \vec{D} .

convergence rate of the error in a suitable norm as the size of interpolation domain, $|\vec{D}|$, tends to zero.

We begin by discussing existence of solutions to (2.6) by looking at the three possible cases, $\mathcal{C}_R > 0$, $\mathcal{C}_R = 0$ and $\mathcal{C}_R < 0$. Existence reduces to investigating the signs of the coefficients in the left hand side of equation (2.6). If $\mathcal{C}_R > 0$, then at least one of the coefficients $(\vec{\alpha} \times \vec{\beta})$, $(\vec{D} \times \vec{\alpha})$, or $(\vec{\beta} \times \vec{D})$ must be positive. Similarly, if $\mathcal{C}_R < 0$, then at least one must be negative. If $\mathcal{C}_R = 0$, then we must have one of each sign, or all must be zero. Within the context of our interpolation problem, if we fail to have existence of solutions to (2.6), then a refinement of the mesh is required until a the existence criteria is met.

We now turn our attention to choosing r_1 and r_2 satisfying (2.6) possessing desirable convergence properties. In particular we are interested in finding r_1 and r_2 which minimize a prescribed distance between the planar curves $\vec{B}(t)$ and $\langle F(s), g(s) \rangle$. Recall that given two parametric curves $\vec{P}_1 : [0, 1] \rightarrow \mathbb{R}^2$ and $\vec{P}_2 : [0, 1] \rightarrow \mathbb{R}^2$, the distance between the sets $P_1, P_2 \in \mathbb{R}^2$ may be measured by the Hausdorff distance

$$(2.7) \quad d_H(P_1, P_2) = \max \left(\sup_{x \in P_1} \inf_{y \in P_2} d(x, y), \sup_{y \in P_2} \inf_{x \in P_1} d(x, y) \right).$$

Here we are seeking the asymptotic decay of $d_H(x, y)$ as the curve lengths tends to zero. In the context of our interpolation problem, for small enough curve length (after rotation if necessary), the target curve is representable by the graph of a function $f(x)$. Therefore, when investigating the accuracy of our interpolating parametric polynomial in this setting we may relax (2.7) to the L^∞ norm

$$(2.8) \quad \|B_2(t) - f(B_1(t))\|_{L^\infty(t \in [0,1])}.$$

Taking the interpolation domain to be $x \in [0, h]$ we search for r_1 and r_2 which satisfy

$$(2.9) \quad \|B_{h_2}(t) - f(B_{h_1}(t))\|_{L^\infty([0,1])} = \mathcal{O}(h^4),$$

where the subscript h signifies that for each choice of $h > 0$ the resulting Bézier interpolant, $\vec{B}(t)$, is generated with potentially different data.

To achieve the above result we employ the method utilized by de Boor et al. in [2] by relying upon classical results for Hermite cubic polynomials $H(x)$. Matching

the data $f(0), f'(0), f(h), f'(h)$ we have $\|H(x) - f(x)\|_{L^\infty([0,h])} = \mathcal{O}(h^4)$, with

$$(2.10) \quad \|H(x) - f(x)\|_{L^\infty([0,h])} \leq \max_{z \in [0,h]} \left| f^{(4)}(z) \right| \frac{h^4}{4!}.$$

To do this, we require that the curve given by $\vec{B}_h(t)$ for $t \in [0, 1]$ can be represented by the graph of a function $b_h(x)$. We show for $0 < r_1, r_2 < 3h$ that $\frac{d}{dt}B_{h_1}(t) > 0$ for $t \in (0, 1)$.

The first of two cases is when we can write $\vec{\alpha} = \langle 1, f'(0) \rangle$. This enables us to write $\frac{d}{dt}B_{h_1}(t)$ as the function

$$(2.11) \quad g(r_1, r_2, t) = t^2(3r_1 + 3r_2 - 6h) + t(-4r_1 - 2r_2 + 6h) + r_1.$$

We show that within the open set $\mathcal{R} = \{(r_1, r_2, t) \in \mathbb{R}^3 \mid (0, 0, 0) < (r_1, r_2, t) < (3h, 3h, 1)\}$ that $g(r_1, r_2, t) > 0$. We first observe that $g(r_1, r_2, t)$ has no critical points in \mathcal{R} , then, checking boundaries and corners of \mathcal{R} , we have values in $[0, 3h]$, implying that the interior has values within $(0, 3h)$, and therefore $g(r_1, r_2, t) > 0$ within the desired region. The second case, when $\vec{\alpha} = \langle 0, 1 \rangle$, yields $\frac{d}{dt}B_{h_1}(t) = 6h(1-t)t$, which is clearly also positive for $t \in (0, 1)$.

Therefore, under the assumption that the target planar curve is the graph of a function $f(x)$, and that $(r_1, r_2, t) \in \mathcal{R}$, we may write

$$(2.12) \quad \|B_{h_2}(t) - f(B_{h_1}(t))\|_{L^\infty([0,1])} = \|b_h(x) - f(x)\|_{L^\infty([0,h])}$$

where the graph of $b_h(x)$ for $x \in [0, h]$ yields the same curve as $\vec{B}_h(t)$ for $t \in [0, 1]$.

Before we proceed we recall that for a parametric function $\langle x(t), y(t) \rangle$, with $x(t)$ and $y(t)$ cubic polynomials, the 4th spacial derivative is given by

$$(2.13) \quad \frac{x' (15(x'')^2 y'' - 4x' x^{(3)} y'' - 6y^{(3)} x' x'') - y' (15(x'')^3 - 10x^{(3)} x' x'')}{(x')^7}.$$

Studying equation (2.13) allows us to prove the following Lemma.

Lemma 2.1. *Suppose $\vec{B}_h(t)$ is interpolating a function $f(x) \in C^4([0, h])$ on $[0, h]$. Then, if $r_1 = h + P_1(h)h^2$ and $r_2 = h + P_2(h)h^2$, where $P_i(h)$ are polynomials in h , then $\vec{B}(t)$ is at least 4th order accurate provided $P_1(h) + P_2(h) = \mathcal{O}(h^q)$ for any $q \geq 1$, or if $f''(0) = 0$.*

Proof. Without loss of generality we assume $\vec{B}_h(0) = \vec{0}$, as discussed previously. The given expression for r_1 and r_2 implies we can find an h small enough to ensure $0 < r_1, r_2 < 3h$, as eventually the leading linear term will dominate, regardless of the values of $P_i(h)$. This guarantees that the graph of $\vec{B}_h(t)$ can be generated by some function $b_h(x)$ for each value of $h > 0$ sufficiently small. The given interpolation problem tells us that $b_h(0) = f(0) = B_{h_2}(0) = 0$, $b_h(h) = f(h) = B_{h_2}(1)$, $g'_h(0) = f'(0) = \frac{B'_{h_2}(0)}{B'_{h_1}(0)}$, and $b'_h(h) = f'(h) = \frac{B'_{h_2}(1)}{B'_{h_1}(1)}$ (The case where the slope at endpoints is infinite can be ignored since further partitioning and rotation can be used). For any given h small enough, the interpolation error is therefore given by

$$e(h) = \|b_h(x) - f(x)\|_{L^\infty[0,h]}.$$

Letting $H(x)$ be the Hermite cubic for $f(x)$ on $x \in [0, h]$, the triangle inequality yields

$$\|b_h(x) - f(x)\|_{L^\infty[0,h]} \leq \|b_h(x) - H(x)\|_{L^\infty[0,h]} + \|H(x) - f(x)\|_{L^\infty[0,h]}.$$

The second term is $\mathcal{O}(h^4)$ by definition of the Hermite polynomial of $f(x)$. We are thus left to show that $\|b_h(x) - H(x)\|_{L^\infty[0,h]}$ is $\mathcal{O}(h^4)$. Since $H(x)$ is also the Hermite cubic polynomial for $b_h(x)$, we apply inequality (2.10) to obtain

$$(2.14) \quad \|b_h(x) - f(x)\|_{L^\infty[0,h]} \leq \sup_{x \in (0,h)} \left| \frac{d^4}{dx^4} b_h(x) \right| \frac{h^4}{4!}.$$

The proof will be complete if $\frac{d^4}{dx^4} b_h(x)$ is bounded as $h \rightarrow 0$. We rely on the property that for each $x \in [0, h]$ there exists a $t^* \in [0, 1]$ such that $\frac{d^4}{dx^4} b_h(x) = \frac{d^3}{dt^3} \left(\frac{B'_{h_2}(t^*)}{B'_{h_1}(t^*)} \right)$. Using equation (2.13) we demonstrate that $\frac{d^3}{dt^3} \left(\frac{B'_{h_2}(t^*)}{B'_{h_1}(t^*)} \right)$ is $\mathcal{O}(1)$ or better. We obtain the desired result by replacing each term by its Taylor expansion, then showing the lowest term in the numerator and denominator are both $\mathcal{O}(h^7)$.

Since we are interpolating a function, after a shift to the origin, the terms from equation (2.2) become $\vec{A} = \vec{0}$, $\vec{D} = \langle h, f(h) \rangle$, $\vec{\alpha} = \langle 1, f'(0) \rangle$, and $\vec{\beta} = \langle 1, f'(h) \rangle$. Starting with

$$\begin{aligned} f(h) &= hf'(0) + \frac{h^2}{2} f''(0) + \mathcal{O}(h^3) \\ f'(h) &= f'(0) + hf''(0) + \frac{h^2}{2} f'''(0) + \mathcal{O}(h^3), \end{aligned}$$

we obtain

$$\begin{aligned} B'_{h_1}(t) &= h + \mathcal{O}(h^2), \quad B''_{h_1}(t) = 2h^2(P_1(h)(-2+3t) + P_2(h)(-1+3t)) + \mathcal{O}(h^3), \\ B'''_{h_1}(t) &= 6h^2(P_1(h) + P_2(h)) + \mathcal{O}(h^3), \\ B'_{h_2}(t) &= f'(0)h + \mathcal{O}(h^2), \\ B''_{h_2}(t) &= 2f'(0)h^2(P_1(h)(-2+3t) + P_2(h)(-1+3t)) + f''(0)h^2 + \mathcal{O}(h^3), \\ B'''_{h_2}(t) &= 6f'(0)h^2(P_1(h) + P_2(h)) + \mathcal{O}(h^3). \end{aligned}$$

In fact, we can simplify our computations further by rewriting the second component derivatives in terms of the first component derivatives, yielding

$$\begin{aligned} B'_{h_2}(t) &= f'(0)B'_{h_1}(t) + \mathcal{O}(h^2), \\ B''_{h_2}(t) &= f'(0)B''_{h_1}(t) + f''(0)h^2 + \mathcal{O}(h^3), \\ B'''_{h_2}(t) &= f'(0)B'''_{h_1}(t) + \mathcal{O}(h^3). \end{aligned}$$

Plugging this into equation (2.13), we obtain

$$\begin{aligned} 15x'(x'')^2 y'' &= 15f'(0)B'_{h_1}(t)(B''_{h_1}(t))^2 \left(B'_{h_1}(t) + \frac{f''(0)}{f'(0)} h^2 \right) = \mathcal{O}(h^7), \\ -4(x')^2 y'' x''' &= -4f'(0)(B'_{h_1}(t))^2 B'''_{h_1}(t) \left(B'_{h_1}(t) + \frac{f''(0)}{f'(0)} h^2 \right) + \mathcal{O}(h^7), \\ -6(x')^2 y''' x'' &= -6f'(0)(B'_{h_1}(t))^2 B''_{h_1}(t) B'''_{h_1}(t) + \mathcal{O}(h^7), \\ -15y'(x'')^3 &= -15f'(0)(B'_{h_1}(t))(B''_{h_1}(t))^3 = \mathcal{O}(h^7), \\ 10y' x' x'' x''' &= 10f'(0)(B'_{h_1}(t))^2 B''_{h_1}(t) B'''_{h_1}(t) + \mathcal{O}(h^7). \end{aligned}$$

Summing each term results in exactly

$$-4f''(0)(B'_{h_1}(t))^2 B''_{h_1}(t)h^2 + \mathcal{O}(h^7) = -4f''(0)h^6(P_1(h) + P_2(h)) + \mathcal{O}(h^7).$$

Therefore, if $P_1(h) + P_2(h) = \mathcal{O}(h^q)$, for $q \geq 1$, or if $f''(0) = 0$, the resulting numerator is at least $\mathcal{O}(h^7)$, which completes the proof. \square

This result gives some direction on how to choose r_1 and r_2 to ensure convergence. In fact, it shows the existence of an entire class of Bézier cubic interpolants which are 4th order accurate or better. However, if we want to prove that a choice of $P_i(h)$ can yield 5th order accuracy or better, then another approach for measuring the error is required.

In the following Lemma we show that there exists a class of $P_i(h)$ which is 5th order accurate or better, provided the curvature doesn't vanish at the endpoints. Later we show that choices of $P_i(h)$ which satisfy the area constraint are within the class of 5th order accurate Bézier cubics.

Lemma 2.2. *Suppose $\vec{B}_h(t)$ is interpolating a function $f(x) \in C^4([0, h])$ on $[0, h]$ with $f''(0) \neq 0$. Then, if $r_1 = h + P_1 h^3$ and $r_2 = h + P_2(h)$, where $P_1 \in \mathbb{R}$, and $P_2(h) = -\frac{f'''(0) + 24f''(0)P_1}{24f''(0)}h^3 + \mathcal{O}(h^4)$ we have $\vec{B}_h(t)$ is at least 5th order accurate.*

Proof. Suppose our Bézier $\vec{B}_h(t) = \langle B_{h_1}(t), B_{h_2}(t) \rangle$, satisfying $B'_{h_1}(t) > 0$ on $t \in (0, 1)$, is interpolating a function $f(x)$ on $x \in [0, h]$, with $f''(0) \neq 0$. Later we will see that for small enough $h > 0$ and given a reasonable choice of P_1 that $B'_{h_1}(t) > 0$ on $t \in (0, 1)$, but for now we leave this as an assumption. To obtain the desired result we work directly with the L^∞ error,

$$(2.15) \quad \|B_{h_2}(t) - f(B_{h_1}(t))\|_{L^\infty(t \in [0, 1])}.$$

Without loss of generality we continue to assume $f(0) = 0$, which implies $B_{h_1}(0) = 0$. We begin by studying the Taylor expansion of $f(B_{h_1}(t))$ centred about $t = 0$,

$$(2.16) \quad \begin{aligned} f(B_{h_1}(t)) &= f'(0)B'_{h_1}(0)t + \left(f''(0)(B'_{h_1}(0))^2 + f'(0)B''_{h_1}(0) \right) \frac{t^2}{2} \\ &\quad + \left(f'''(0)(B'_{h_1}(0))^3 + 3f''(0)B''_{h_1}(0)B'_{h_1}(0) + f'(0)B'''_{h_1}(0) \right) \frac{t^3}{6} \\ &\quad + \left(f''''(0)(B'_{h_1}(0))^4 + 3f''(0)(B''_{h_1}(0))^2 + 4f''(0)B'_{h_1}(0)B'''_{h_1}(0) + 6f'''(0)B''_{h_1}(0)(B'_{h_1}(0))^2 \right) \frac{t^4}{24} \\ &\quad + \mathcal{O}(t^5), \end{aligned}$$

$$\text{where } B_{h_1}(t) = (h + P_1 h^3)t - (P_2(h) + 2P_1 h^3)t^2 + (P_1 h^3 + P_2(h))t^3.$$

Plugging this into (2.16) yields

$$\begin{aligned} f(B_{h_1}(t)) &= (h + P_1 h^3)f'(0)t + \left(f''(0)(h + P_1 h^3)^2 - 2f'(0)(P_2(h) + 2P_1 h^3) \right) \frac{t^2}{2} \\ &\quad + \left(f'''(0)(h + P_1 h^3)^3 - 6f''(0)(P_2(h) + 2P_1 h^3)(h + P_1 h^3) + 6f'(0)(P_1 h^3 + P_2(h)) \right) \frac{t^3}{6} \\ &\quad + \mathcal{O}(t^4). \end{aligned}$$

Dropping terms which are $\mathcal{O}(h^5)$ or higher results in

$$\begin{aligned} f(B_{h_1}(t)) &= (h + P_1 h^3) f'(0) t + \left(f''(0)(h^2 + 2P_1 h^4) - 2f'(0)(P_2(h) + 2P_1 h^3) \right) \frac{t^2}{2} \\ &\quad + \left(f'''(0)h^3 - 6f''(0)(hP_2(h) + 2P_1 h^4) + 6f'(0)(P_1 h^3 + P_2(h)) \right) \frac{t^3}{6} \\ &\quad + \left(f''''(0)h^4 + 24f''(0)(P_1 h^4 + P_2(h)h) \right) \frac{t^4}{24} + \mathcal{O}(t^5). \end{aligned}$$

We proceed to show for any choice of $P_1 \in \mathbb{R}$ that taking

$$P_2(h) = -\frac{f''''(0) + 24f''(0)P_1}{24f''(0)} h^3 + \mathcal{O}(h^4) \text{ yields } \|B_{h_2}(t) - f(B_{h_1}(t))\|_{L^\infty(t \in [0,1])} = \mathcal{O}(h^5). \text{ Recalling our equation for } B_{h_2}(t),$$

$$\begin{aligned} B_{h_2}(t) &= \mathcal{H}_2(t) + f'(0)P_1 h^3 t - \left(f'(h)P_2(h) + 2f'(0)P_1 h^3 \right) t^2 + (f'(0)P_1 h^3 + f'(h)P_2(h)) t^3 \\ &= (h + P_1 h^3) f'(0) t + \left(3f(h) - 2hf'(0) - hf'(h) - f'(h)P_2(h) - 2f'(0)P_1 h^3 \right) t^2 \\ &\quad + \left(hf'(0) + hf'(h) - 2f(h) + f'(0)P_1 h^3 + f'(h)P_2(h) \right) t^3. \end{aligned}$$

Taylor expanding $f(h)$ and $f'(h)$ up to $\mathcal{O}(h^5)$ and dropping terms which are $\mathcal{O}(h^5)$ or higher, $B_{h_2}(t)$ simplifies to

$$\begin{aligned} B_{h_2}(t) &= (h + P_1 h^3) f'(0) t + \left(f''(0) \frac{h^2}{2} - f''''(0) \frac{h^4}{24} - (f'(0) + hf''(0)) P_2(h) - 2f'(0) P_1 h^3 \right) t^2 \\ (2.17) \quad &\quad + \left(f'''(0) \frac{h^3}{6} + f''''(0) \frac{h^4}{12} + f'(0) P_1 h^3 + (f'(0) + hf''(0)) P_2(h) \right) t^3. \end{aligned}$$

Using (2.17) and (2.16) we can compute $\|B_{h_2}(t) - f(B_{h_1}(t))\|_{L^\infty(t \in [0,1])}$. Going term by term we have

$$\begin{aligned} |B_{h_2}(t) - f(B_{h_1}(t))| &\leq \left| (h + P_1 h^3) - (h + P_1 h^3) \right| t \\ &\quad + \left| -f''(0)(hP_2(h) + P_1 h^4) - f''''(0) \frac{h^4}{24} \right| t^2 \\ &\quad + \left| f''''(0) \frac{h^4}{12} + f''(0)(2hP_2(h) + 2P_1 h^4) \right| t^3 \\ &\quad + \left| f''''(0) \frac{h^4}{24} + f''(0)(P_1 h^4 + P_2(h)h) \right| t^4 + \mathcal{O}(h^5) + \mathcal{O}(t^5) \end{aligned}$$

Setting $P_2(h) = -\frac{f''''(0) + 24f''(0)P_1}{24f''(0)} h^3 + \mathcal{O}(h^4)$ we obtain the desired result that $|B_{h_2}(t) - f(B_{h_1}(t))| = \mathcal{O}(h^5)$. \square

Remark 2.3. We note that the $\mathcal{O}(t^5)$ terms do not contribute any terms lower than h^5 , because each time we differentiate a term of the form $f^{(n_1)}(0)(B'_{h_1}(0))^{n_2}(B''_{h_1}(0))^{n_3}(B'''_{h_1}(0))^{n_4}$, for $n_i \in \mathbb{N}$ the lowest power of h must increase since $B'_{h_1}(0) = \mathcal{O}(h)$, $B''_{h_1}(0) = \mathcal{O}(h^2)$ and $B'''_{h_1}(0) = \mathcal{O}(h^3)$.

With Lemmas 2.1 and 2.2 in hand, we may now state our main result.

Theorem 2.4. *Parametric area-preserving Bézier cubics, satisfying $B'_1(0) = r_1 = h + Ph^3$, for $P \in \mathbb{R}$, and $B'_1(1) = r_2 = \frac{6(10Cr - r_1(\vec{B}^* \times \vec{\alpha}))}{r_1(\vec{\alpha} \times \vec{\beta}) + 6(\vec{\beta} \times \vec{B}^*)}$, are 5th order accurate*

provided the curvature is non-vanishing at endpoints. In the zero curvature case, the interpolation is 4th order accurate.

Proof. We begin by proving the non-zero curvature case, which simply breaks down into showing that setting $r_1 = h + Ph^3$ and $r_2 = \frac{6(10Cr - r_1(\vec{B}^* \times \vec{\alpha}))}{r_1(\vec{\alpha} \times \vec{\beta}) + 6(\vec{\beta} \times \vec{B}^*)}$ satisfies the conditions from Lemma 2. Again, since we are seeking the error as $h \rightarrow 0$, we will assume that we are interpolating a function $f(x)$ on $[0, h]$. Inputing the data from $f(x)$ into the given equation for r_2 yields

$$(2.18) \quad r_2 = \frac{6 \left(10 \left(\int_0^h f(x) dx - \frac{hf(h)}{2} \right) - (h + Ph^3) (\langle h, f(h) \rangle \times \langle 1, f'(0) \rangle) \right)}{(h + Ph^3) (\langle 1, f'(0) \rangle \times \langle 1, f'(h) \rangle) + 6 (\langle 1, f'(h) \rangle \times \langle h, f(h) \rangle)}$$

$$= \frac{6 \left(10 \left(\int_0^h f(x) dx - \frac{hf(h)}{2} \right) - (h + Ph^3) (hf'(0) - f(h)) \right)}{(h + Ph^3) (f'(h) - f'(0)) + 6 (f(h) - hf'(h))}.$$

Plugging in the Taylor expansion for each term in (2.18), we obtain

$$(2.19) \quad r_2 = \frac{-2f''(0)h^3 - \frac{3}{2}f'''(0)h^4 + (3f''(0)P - \frac{1}{2}f''''(0))h^5 + \mathcal{O}(h^6)}{-2f''(0)h^2 - \frac{3}{2}f'''(0)h^3 + (f''(0)P - \frac{7}{12}f''''(0))h^4 + \mathcal{O}(h^5)},$$

which, for small enough $h > 0$ is equivalent to

$$(2.20) \quad r_2 = h - \frac{f''''(0) + 24f''(0)P}{24f''(0)}h^3 + \mathcal{O}(h^4).$$

Therefore, by Lemma 2, we have our result.

In the case that $f''(0) = 0$, we follow a similar approach. Taking a Taylor expansion in x of each term in r_2 we obtain

$$(2.21) \quad r_2 = \frac{-\frac{3}{2}f''''(0)h^4 + -\frac{1}{2}f''''(0)h^5 + \mathcal{O}(h^6)}{-\frac{3}{2}f''''(0)h^3 + -\frac{7}{12}f''''(0)h^4 + \mathcal{O}(h^5)},$$

which, for small enough $h > 0$, is equivalent to

$$r_2 = h - \frac{f''''(0)}{18f''''(0)}h^2 + \mathcal{O}(h^3).$$

Therefore, by Lemma 1, since $r_1 = h + Ph^3$ and $r_2 = h + P_2(h)h^2$, for $P_2(h)$ a polynomial and $f''(0) = 0$, we have that the curvature vanishing case is 4th order accurate. \square

A simple computation leads us to the following Corollary on optimality.

Corollary 2.5. *There does not exist a 6th order Bézier cubic area-preserving interpolating polynomial.*

Proof. Suppose we allow the constant P_1 to be a function of h , yielding $r_1 = h + P_1(h)h^3$, with $r_2 = \frac{6(10Cr - r_1(\vec{B}^* \times \vec{\alpha}))}{r_1(\vec{\alpha} \times \vec{\beta}) + 6(\vec{\beta} \times \vec{B}^*)}$ to guarantee area preservation. Applying a Taylor expansion on the error (2.15) we obtain

$$\|B_{h_2}(t) - f(B_{h_1}(t))\|_{L^\infty(t \in [0,1])} = \frac{(5f''''(0)f''''(0) - 2f''(0)f''''(0))(4t - 1)t^2}{480f''(0)}h^5 + \mathcal{O}(h^6, t^4).$$

Observing that the h^5 term does not contain a $P_1(h)$ implies the only way to obtain 6th order would be to have $P_2(h) \approx \frac{1}{h}$, to allow the h^6 term to cancel out the h^5 term. This is equivalent to setting $r_1 = h + P_1(h)h^2$, however, this leads to a

complicated h^5 term containing the time variable t . Therefore since we require $P_1(h)$ to not vary with t , no order higher than h^5 is possible. \square

The following Corollary proves that if we are unable to provide an exact area, but instead an approximate area up to some order $\mathcal{O}(h^5)$, that the L^∞ error drops to $\mathcal{O}(h^4)$.

Corollary 2.6. *If the prescribed area is an approximation of the true area with order $\mathcal{O}(h^5)$, then the area-preserving Bézier interpolation discussed above satisfies $\|B_{h_2}(t) - f(B_{h_1}(t))\|_{L^\infty(t \in [0,1])} = \mathcal{O}(h^4)$.*

Proof. Suppose the prescribed area is not exact with error $\mathcal{O}(h^5)$. This changes equation (2.6) to

$$(2.22) \quad \frac{r_1 r_2}{60} (\vec{\alpha} \times \vec{\beta}) + \frac{r_1}{10} (\vec{D} \times \vec{\alpha}) + \frac{r_2}{10} (\vec{\beta} \times \vec{D}) = C_R + Mh^5 + \mathcal{O}(h^6),$$

for h small enough, where $M \in \mathbb{R}$ is some constant independent of h . Solving for r_2 yields

$$r_2 = \frac{6(10Cr + Mh^5 + \mathcal{O}(h^6)) - r_1(\vec{B}^* \times \vec{\alpha})}{r_1(\vec{\alpha} \times \vec{\beta}) + 6(\vec{\beta} \times \vec{B}^*)}.$$

Repeating the steps from Theorem 2.4, with $r_1 = h + Ph^3$, we now obtain

$$r_2 = h - \frac{f''''(0) + 24f''(0)P + 720M}{24f''(0)} h^3 + \mathcal{O}(h^4).$$

This results in $r_1 = h + \mathcal{O}(h^3)$ and $r_2 = h + \mathcal{O}(h^3)$ which satisfies the conditions for Lemma 1, implying 4th order accuracy. \square

3. NUMERICAL RESULTS

3.1. Preliminary Considerations. In this section we present several examples illustrating the effectiveness of exact area-preserving Bézier cubic interpolation. For a few of these examples we employ two methods. First we use the standard choice of $r_1 = h + Ph^3$, where P is chosen a priori. We also employ an optimized method, where r_1 and r_2 are chosen to numerically minimize the error by extracting additional information from the target function. For the standard scheme we assign P to be P_{avg} , given by

$$(3.1) \quad P_{avg} = \frac{1}{h^3} \left[\frac{1}{2} \left(h + \frac{6(10Cr - h(\vec{\beta} \times \vec{B}^*))}{h(\vec{\alpha} \times \vec{\beta}) + 6(\vec{B}^* \times \vec{\alpha})} \right) - h \right].$$

We arrive at P_{avg} by taking the average of $r_1 = h$ and

$r_1 = \frac{6(10Cr - h(\vec{\beta} \times \vec{B}^*))}{h(\vec{\alpha} \times \vec{\beta}) + 6(\vec{B}^* \times \vec{\alpha})}$, which arises by solving the area equation for r_1 instead of r_2 and simply setting $r_2 = h$. A similar computation as in the proof of Theorem 2.4, shows that $\frac{6(10Cr - h(\vec{\beta} \times \vec{B}^*))}{h(\vec{\alpha} \times \vec{\beta}) + 6(\vec{B}^* \times \vec{\alpha})} = h - \frac{f''''(0)}{24f''(0)} h^3 + \mathcal{O}(h^4)$. Plugging this into the equation for P_{avg} we see that $P_{avg} = \mathcal{O}(1)$ as desired.

The standard scheme described above is an efficient 5th order method which, in most cases, performs remarkably well. However, there are choices of r_1 which lead to greater precision, but they are problem specific and require an iterative process to compute. In many applications this additional precision may not be necessary,

however it is important to note that more optimal choices of r_1 and r_2 can be obtained.

We therefore seek solutions to the optimization problem

$$(3.2) \quad \min_{(r_1, r_2) \in \mathcal{S}} \|B_{h_2}(t, r_1, r_2(r_1)) - f(B_{h_1}(t, r_1, r_2(r_1)))\|_{L^\infty(t \in [0, 1])},$$

where \mathcal{S} is the set of all $(r_1, r_2) > 0$ which results in a Bézier cubic representable by a function $b(x)$. We note that an exact representation of \mathcal{S} is easily obtained, however the square $0 < r_1, r_2 \leq 3h$ does sufficiently well.

We implement the optimized method by discretizing $0 < r_1 \leq 3h$ into a fine grid $0 < r_{1_1} < r_{1_2} < \dots < r_{1_n} = 3h$, then compute $r_2(r_{1_i})$. For each pair $(r_{1_i}, r_2(r_{1_i})) \in \mathcal{S}$ we approximate the norm (3.2) then choose the minimizer amongst all candidates. We note that if the target curve is a parametric curve $\langle F(s), g(s) \rangle$, then we replace (3.2) with the Hausdorff distance (2.7).

In the remaining subsections we will illustrate our theoretical findings through numerical examples. We present convergence in the L^∞ norm, but do not include any discussion of the error in the area, as, by construction, it was found to be machine precision in all examples.

3.2. Example 1: Unit Circle. Our first example is repeating the first example in section 4 of [2], interpolating the unit circle. We instead interpolate the semi circle as our scheme is rotation invariant, and measure the L^∞ error as we partition the semi circle into subintervals with decreasing length. Beginning with 2 sub intervals, or 4 points over the entire circle up to 32 points over the entire circle, or partitioning the semi circle into 16 subintervals. At each step we compare the L^∞ error obtained by our area-preserving scheme versus the (non-area preserving) curvature matching scheme in [2]. The results are shown in Table 1. The results show that the curvature

Number of points	Curvature Matching [2]	Area-Preserving	Optimized Area-Preserving
4	1.4×10^{-3}	2.9×10^{-3}	2.6×10^{-4}
8	2.1×10^{-5}	5.7×10^{-5}	4.5×10^{-6}
16	3.2×10^{-7}	1.0×10^{-6}	8.2×10^{-8}
32	4.9×10^{-9}	1.6×10^{-8}	3.3×10^{-9}

TABLE 1. L^∞ error of area-preserving versus curvature matching.

matching and standard area-preserving methods are quite close through 16 points. We see the curvature method nudging ahead at 32 points, which isn't surprising as it is a 6th order method. The optimized approach however is significantly more accurate than the others with between 10 and 20 times the accuracy through sixteen points. At 32 points the error is comparable to the curvature method. Figure 2 confirms that the convergence is indeed 5th order, agreeing with the statement of Theorem 2.4.

3.3. Vanishing Curvature. The following example illustrates the statement of Theorem 2.4 when we have vanishing curvature. The target function is $f(x) = \sin(x) + 3x^4 - 4x^3 + x$ for $x \in [0, h]$, and the resulting convergence using P_{avg} defined in section 3.1 is given in Figure 3. As predicted we obtain 4th order accuracy, the same as would be obtained by employing the method of de Boor et al. As we are

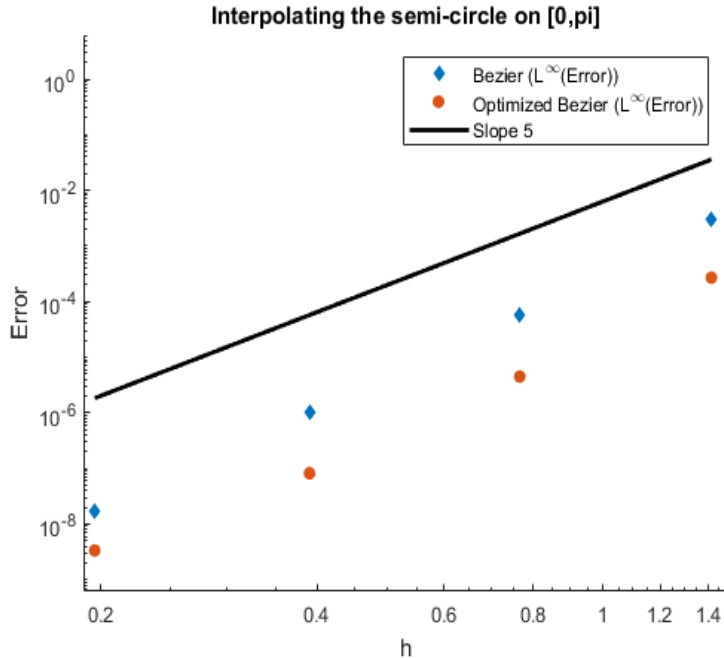


FIGURE 2. Illustrating 5th order convergence when interpolating the unit circle.

only illustrating the 4th order accuracy of the method in the presence of vanishing curvature, we do not discuss the optimized approach in this problem.

3.4. Comparison to the CVE method. To get a sense of how the standard area-preserving geometric interpolation method compares to other non-local G^1 methods, we repeat the last example from [11], the method which minimizes an approximate curvature variation energy. In this example we are interpolating the parametric curve

$$(3.3) \quad \vec{f}(t) = \langle (t^3 - t + 1) \sin(t), t \cos(t) \rangle \quad \text{for } t \in [0, 1].$$

The function (3.3) is broken up into two subintervals $[0, 0.3678]$ and $[0.3678, 1]$ in the first example, and $[0, 0.48]$ and $[0.48, 1]$ in the second. The plot of the resulting interpolations are shown in Figure 4. Since (3.3) is a parametric function, we estimate the error by approximating the Hausdorff distance by partitioning the interpolant and $\vec{f}(t)$ and computing (2.7) discretely. The results are given in Table 2. We note that the Hausdorff errors for the CVE method were not included in [11], so it needed to be approximated from their Figure 5 and Figure 6. The results in Table 2 show us that between 10 and 40 times the accuracy may be gained when using the standard area-preserving method over the Curvature Variation Energy method of [11].

3.5. Optimized Area-Preservation. In this next example we showcase the accuracy that may be gained by selecting optimized r_1 and r_2 . We interpolate the function $f(x) = 4x(x - 0.5)(x - 1)e^x$ on the interval $x \in [0, 1]$. Figure 5 shows $f(x)$,

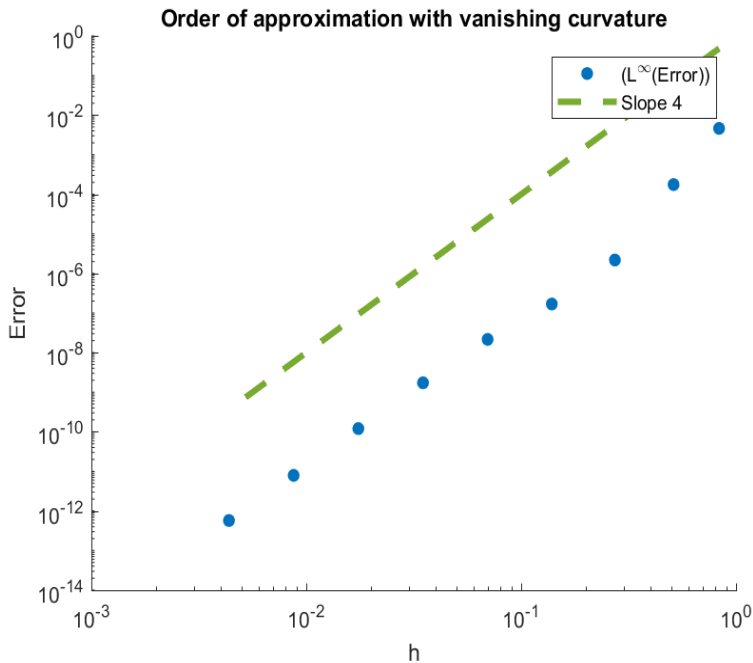


FIGURE 3. Example of 4th order accuracy with vanishing curvature.

Interpolation intervals	CVE [11]	Area-Preserving
[0,0.3678] and [0.36,1]	$\approx 3 \times 10^{-2}$	6.9×10^{-4}
[0,0.48] and [0.48,1]	$\approx 2 \times 10^{-2}$	2.4×10^{-3}

TABLE 2. Approximate Hausdorff error of CVE method of [11] versus the area-preserving method.

the Hermite interpolant, the standard area-preserving Bézier with $P = 0$ and then the optimized area-preserving Bézier. We note that Figure 5 appears to only have 3 curves because the optimized curves is nearly identical to the target function $f(x)$.

3.6. Piecewise Interpolation I. In the next example we construct a piecewise interpolation of the function $f(x) = (x + 1)e^x - 1$ on the interval $[0, 1]$. We partition the domain into finer and finer subintervals, compute the interpolants on each subinterval, then compute the maximum L^∞ error over all interpolants. Figure 6 shows the L^∞ error convergence for Hermite interpolation, area-preserving Bézier interpolation with $(r_1, r_2) = (h, r_1(h))$ and the optimized choice (r_{1_i}, r_{2_i}) described in section 3.1.

Figure 6 showcases the 5th order convergence of the standard area-preserving method with $r_1 = h$, shown in blue, and the 4th order convergence of the Hermite polynomial. The dramatic improvement of the optimized curve is also visible as in Figure 5, but the convergence is less consistent.

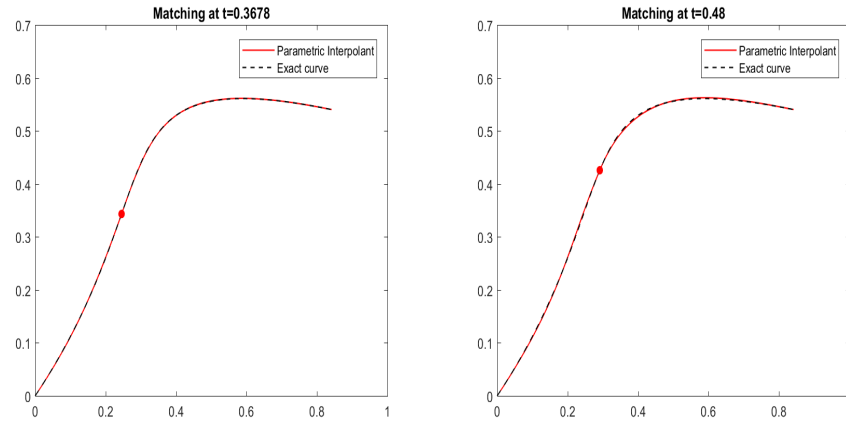


FIGURE 4. Two area-preserving G^1 polynomials interpolate (3.3) joining at $t = 0.3678$ on the left panel and $t = 0.48$ on the right panel.

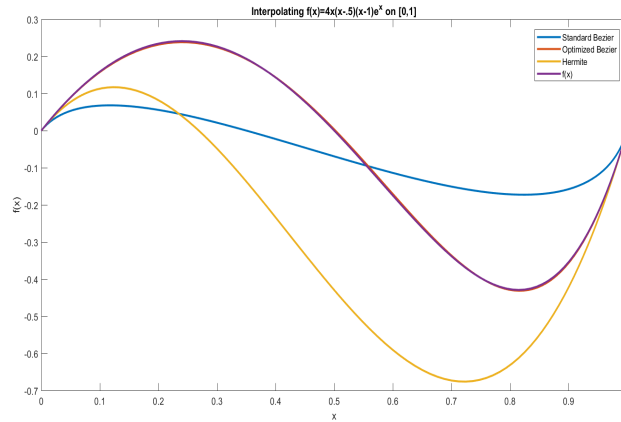


FIGURE 5. Interpolation of $f(x) = 4x(x - 0.5)(x - 1)e^x$.

3.7. Piecewise Interpolation II. The last example has the same set up as the previous, but now the target function is $f(x) = x^2(1 - x)e^x$. The significance of this example is that $f(x)$ has an inflection point, therefore by Theorem 2.4 we expect to obtain 4^{th} order convergence. The results are shown in in Figure 7. We see that both the optimized and unoptimized methods are 4^{th} order accurate by observing the last few data points. The inconsistency of the optimized convergence is simply a result of where the grid points land relative to the inflection point and areas with high curvature.

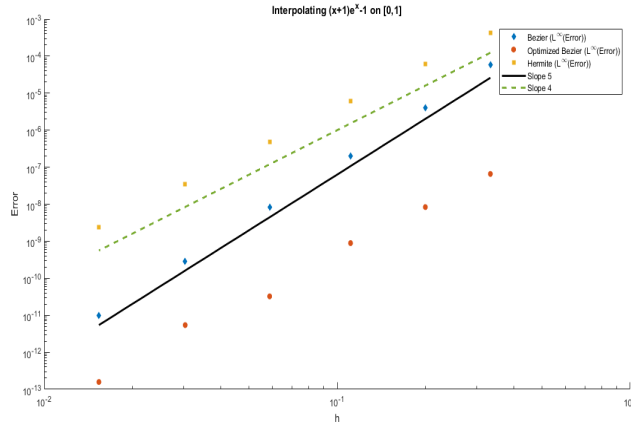


FIGURE 6. 5th order convergence of standard area-preserving method and optimized method.

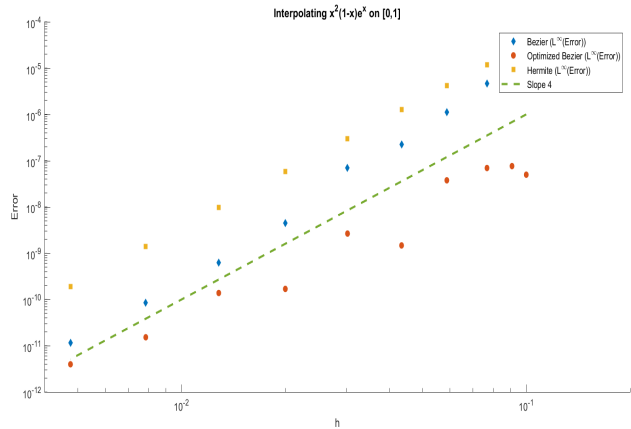


FIGURE 7. 4th order convergence of standard area-preserving method and optimized method when an inflection point is present within interpolation domain.

4. DISCUSSION

In this paper we set out to design a new Bézier cubic interpolation framework which exactly preserves area while maintaining high accuracy. Theorem 2.4 demonstrates that, provided we select r_1 correctly, matching the prescribed area with a geometric Hermite cubic polynomial yields 5th order accuracy, one order higher than the standard geometric Hermite. This order is optimal for area-preserving cubics as shown in Corollary 2.5. In section 3 we verify numerically the statements of Theorem 2.4 by obtaining 5th order accuracy when the curvature is non-vanishing and 4th order otherwise. The numerical comparisons with the methods of [2] and [11] show that the our area-preserving method is competitive or superior in the L^∞

or Hausdorff error, with the area-preserving method offering the additional benefit of being conservative. The optimized method discussed at the end of the results section shows that further improvements to accuracy can be obtained when an iterative process to find an optimal choice of r_1 and r_2 is employed. In the near future we look forward to applying this framework to numerical methods for conservation laws and gradient augmented level set methods, such as those discussed in [16, 17].

REFERENCES

1. Brian A Barsky and Tony D DeRose, *Geometric continuity of parametric curves: three equivalent characterizations*, IEEE Computer Graphics and Applications **9** (1989), no. 6, 60–69.
2. Carl De Boor, Klaus Höllig, and Malcolm Sabin, *High accuracy geometric hermite interpolation*, Computer Aided Geometric Design **4** (1987), no. 4, 269–278.
3. Gerald Farin, *Curves and surfaces for computer-aided geometric design: a practical guide*, Elsevier, 2014.
4. Rida T Farouki, *Pythagorean hodograph curves in practical use*, Geometry processing for design and manufacturing, SIAM, 1992, pp. 3–33.
5. ———, *Construction of $g1$ planar hermite interpolants with prescribed arc lengths*, Computer Aided Geometric Design **46** (2016), 64–75.
6. Rida T Farouki, Mohammad al Kandari, and Takis Sakkalis, *Hermite interpolation by rotation-invariant spatial pythagorean-hodograph curves*, Advances in Computational Mathematics **17** (2002), no. 4, 369–383.
7. Rida T Farouki, Carlotta Giannelli, Carla Manni, and Alessandra Sestini, *Identification of spatial ph quintic hermite interpolants with near-optimal shape measures*, Computer Aided Geometric Design **25** (2008), no. 4-5, 274–297.
8. Rida T Farouki and C Andrew Neff, *Hermite interpolation by pythagorean hodograph quintics*, Mathematics of computation **64** (1995), no. 212, 1589–1609.
9. John A Gregory, *Geometric continuity*, Mathematical methods in computer aided geometric design, Elsevier, 1989, pp. 353–371.
10. Klaus Höllig and Jürgen Koch, *Geometric hermite interpolation with maximal order and smoothness*, Computer Aided Geometric Design **13** (1996), no. 8, 681–695.
11. Gašper Jaklič and Emil Žagar, *Curvature variation minimizing cubic hermite interpolants*, Applied Mathematics and Computation **218** (2011), no. 7, 3918–3924.
12. ———, *Planar cubic $g1$ interpolatory splines with small strain energy*, Journal of computational and applied mathematics **235** (2011), no. 8, 2758–2765.
13. Randall J LeVeque, *Numerical methods for conservation laws*, vol. 132, Springer, 1992.
14. Lizheng Lu, *Planar quintic $g2$ hermite interpolation with minimum strain energy*, Journal of Computational and Applied Mathematics **274** (2015), 109–117.
15. Lizheng Lu, Chengkai Jiang, and Qianqian Hu, *Planar cubic $g1$ and quintic $g2$ hermite interpolations via curvature variation minimization*, Computers & Graphics **70** (2018), 92–98.
16. Jean-Christophe Nave, Rodolfo Ruben Rosales, and Benjamin Seibold, *A gradient-augmented level set method with an optimally local, coherent advection scheme*, Journal of Computational Physics **229** (2010), no. 10, 3802–3827.
17. Benjamin Seibold, Jean-Christophe Nave, and Rodolfo Ruben Rosales, *Jet schemes for advection problems*, arXiv preprint arXiv:1101.5374 (2011).
18. Andy TS Wan and Jean-Christophe Nave, *On the arbitrarily long-term stability of conservative methods*, SIAM Journal on Numerical Analysis **56** (2018), no. 5, 2751–2775.
19. Jun-Hai Yong and Fuhua Frank Cheng, *Geometric hermite curves with minimum strain energy*, Computer Aided Geometric Design **21** (2004), no. 3, 281–301.

DEPARTMENT OF MATHEMATICS, MCGILL UNIVERSITY, MONTREAL, QC, CANADA.

Current address: 805 Sherbrooke St W, Montreal, QC H3A 0B9, Canada.

E-mail address: Geoffrey.McGregor@mail.mcgill.ca

DEPARTMENT OF MATHEMATICS, MCGILL UNIVERSITY, MONTREAL, QC, CANADA.

E-mail address: jcnave@math.mcgill.ca